

Effects of vacuum-ultraviolet irradiation on copper penetration into low-k dielectrics under bias-temperature stress

X. Guo, S. W. King, H. Zheng, P. Xue, Y. Nishi, and J. L. Shohet

Citation: [Applied Physics Letters](#) **106**, 012904 (2015); doi: 10.1063/1.4905462

View online: <http://dx.doi.org/10.1063/1.4905462>

View Table of Contents: <http://scitation.aip.org/content/aip/journal/apl/106/1?ver=pdfcov>

Published by the [AIP Publishing](#)

Articles you may be interested in

[Effect of vacuum-ultraviolet irradiation on the dielectric constant of low-k organosilicate dielectrics](#)

Appl. Phys. Lett. **105**, 202902 (2014); 10.1063/1.4901742

[Effects of plasma and vacuum-ultraviolet exposure on the mechanical properties of low-k porous organosilicate glass](#)

J. Appl. Phys. **116**, 044103 (2014); 10.1063/1.4891501

[Bandgap measurements of low-k porous organosilicate dielectrics using vacuum ultraviolet irradiation](#)

Appl. Phys. Lett. **104**, 062904 (2014); 10.1063/1.4865407

[The effects of plasma exposure and vacuum ultraviolet irradiation on photopatternable low-k dielectric materials](#)

J. Appl. Phys. **114**, 104107 (2013); 10.1063/1.4821065

[Cu penetration into low- k dielectric during deposition and bias-temperature stress](#)

Appl. Phys. Lett. **97**, 252901 (2010); 10.1063/1.3529492

The logo for Applied Physics Letters (AIP) is displayed in a white font on an orange background. The letters 'AIP' are large and bold, followed by a vertical bar and the words 'Applied Physics Letters' in a smaller font.

Meet The New Deputy Editors



Alexander A.
Balandin



Qing Hu



David L.
Price

Effects of vacuum-ultraviolet irradiation on copper penetration into low-k dielectrics under bias-temperature stress

X. Guo,¹ S. W. King,² H. Zheng,¹ P. Xue,¹ Y. Nishi,³ and J. L. Shohet¹

¹Plasma Processing & Technology Laboratory and Department of Electrical and Computer Engineering, University of Wisconsin-Madison, Madison, Wisconsin 53706, USA

²Logic Technology Development, Intel Corporation, Hillsboro, Oregon 97124, USA

³Department of Electrical Engineering, Stanford University, Stanford, California 94305, USA

(Received 16 October 2014; accepted 21 December 2014; published online 6 January 2015)

The effects of vacuum-ultraviolet (VUV) irradiation on copper penetration into non-porous low-k dielectrics under bias-temperature stress (BTS) were investigated. By employing x-ray photoelectron spectroscopy depth-profile measurements on both as-deposited and VUV-irradiated SiCOH/Cu stacks, it was found that under the same BTS conditions, the diffusion depth of Cu into the VUV-irradiated SiCOH is higher than that of as-deposited SiCOH. On the other hand, under the same temperature-annealing stress (TS) without electric bias, the Cu distribution profiles in the VUV-irradiated SiCOH were same with that for the as-deposited SiCOH. The experiments suggest that in as-deposited SiCOH, the diffused Cu exists primarily in the atomic state, while in VUV-irradiated SiCOH, the diffused Cu is oxidized by the hydroxyl ions (OH^-) generated from VUV irradiation and exists in the ionic state. The mechanisms for metal diffusion and ion injection in VUV irradiated low-k dielectrics are discussed. © 2015 AIP Publishing LLC.

[<http://dx.doi.org/10.1063/1.4905462>]

To prevent increased resistance-capacitance delays and capacitive-power dissipation, back-end-of-the-line (BEOL) dielectrics with low dielectric constants (i.e., k) and advanced Cu interconnect structures are needed for current and future integrated circuit technology.¹ However, the required reduced- k -value of the interlayer dielectrics (ILDs), typically produced by the introduction of nanoporosities, can seriously compromise the performance of an actual low- k /Cu interconnect.^{2,3} The penetration of Cu into a low- k dielectric can cause serious reliability issues, and it is increasingly more challenging to contain Cu within lines due to the aggressive shrinking of the interconnect pitch. Continuous technology scaling may eventually expose Cu to the low- k dielectrics directly. Thus, the stability of Cu/low- k dielectric interfaces has become an even more pressing issue.

As a result, copper-diffusion-induced instabilities have become a crucial impediment to successful integration of low- k dielectrics with Cu interconnects and has generated extensive interest in understanding the mechanisms of Cu diffusion into the low- k ILDs. Research is currently focused on Cu diffusion into as-deposited low- k dielectrics. This issue, however, has received only minimal attention for vacuum-ultraviolet (VUV) photon-irradiated low- k dielectrics. Usually, microprocessor units (MPUs) have more than 20 layers of interconnects,⁴ and thus, the ILDs will be constantly exposed to VUV photons generated from repeated plasma etching and deposition processes during fabrication. VUV photon irradiation has to be considered when studying the Cu/low- k interconnect reliability issue. Previous work has demonstrated that it can affect the breakdown voltage,⁵ leakage current,⁶ capacitance,⁷ and the time-dependent dielectric breakdown (TDDB) lifetimes of these materials significantly.^{8,9}

In this letter, to evaluate the effect of VUV irradiation on Cu penetration into low- k dielectrics under bias-temperature stress (BTS), we have utilized x-ray photoelectron spectroscopy (XPS) depth profiling strategies to determine and compare the Cu distribution profiles in as-deposited and VUV-irradiated samples. The low- k dielectric used here is plasma-enhanced chemical-vapor deposited (PECVD) *nonporous* SiCOH with a dielectric constant of ~ 3.2 and a density of 1.5 g/cm^3 . Instead of depositing Cu electrodes on the surface of low- k SiCOH thin films, the sample preparation procedure is optimized by employing PECVD deposition of SiCOH on polished Cu thin-film substrates, because Cu was found to diffuse into the dielectric layer during depositing Cu electrodes onto the SiCOH using either e-beam evaporation or sputter deposition.¹⁰

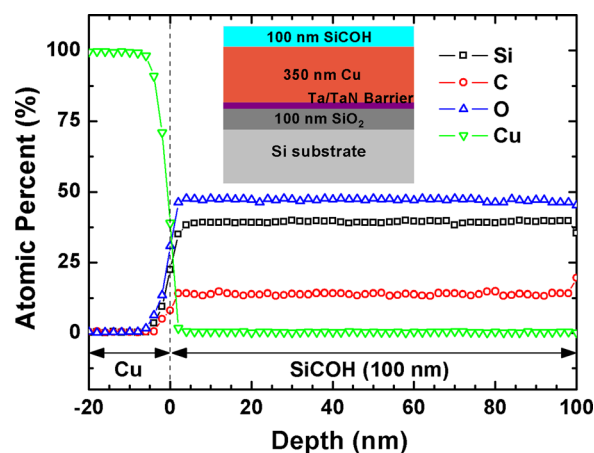


FIG. 1. XPS depth profile of the as-deposited SiCOH without bias temperature stressing (BTS). Inset shows the schematics of the sample structure utilized in this work.

The inset in Figure 1 shows the schematic of the SiCOH/Cu stack-structure utilized in this work, which is designed to minimize the electrode-deposition-induced Cu penetration into the dielectrics. First, the Cu was electrochemically plated (ECP) on a Cu seed and a TaN adhesion layer sputter-deposited on a 300-mm diameter (100) Si substrate on which 100 nm of thermal oxide had been previously grown. After that, the ECP Cu was chemically mechanically polished (CMP) to 350 nm. Prior to SiCOH deposition, H₂ plasma pre-treatment was performed *in-situ* to remove Cu corrosion inhibitors left behind by the Cu CMP process and to reduce Cu surface oxides formed by ambient exposure. Finally, the SiCOH thin films were deposited at a thickness of 100 nm on the Cu film at temperatures on the order of 400 °C using a standard commercially available 300-mm PECVD tool. The XPS depth profile of the chemical components, as shown in Figure 1, reveals that no detectable Cu exists in the as-deposited SiCOH films fabricated using the procedure described above. Additional details concerning the PECVD processing and thin film measurements have been previously reported.^{11,12} It should be mentioned that no organic pore building “porogen” was used during the ILD deposition and no e-beam or UV cure was utilized after deposition. This inhibits moisture uptake of the samples by significantly reducing the concentration of the hydrophilic groups from porogen residuals in the dielectric.

Subsequently, monochromatic VUV radiation exposures were made at the UW-Madison Synchrotron Radiation facility using a system described previously.¹³ The VUV photon energy was set at 9.0 eV (137 nm), because the reported penetration depth at these photon energies through amorphous silica-based dielectrics has been estimated to be ~200 nm,¹⁴ which is larger than the thickness of the SiCOH thin films used here. Consequently, the entire bulk of the low-k dielectrics can be chemically modified with 9.0 eV VUV photon irradiation. The photon flux was monitored *in-situ* using a calibrated photodiode (AXUV100) and the total photon fluence impinging on the sample was approximately 4.0×10^{15} photons/cm². This value is comparable to the total UV/VUV photon fluence emitted during a typical “downstream” ECR plasma exposure.¹³ The temperature of the dielectric film was monitored with a thermocouple connected to the back of the sample and did not show significant changes during the VUV irradiation. The photoemission current and substrate current were also recorded.

After VUV irradiation, the film thickness and density of the samples were measured using a three-color ellipsometer and X-ray reflectivity, respectively. It should be noted that after VUV irradiation, to avoid exposing the samples to ambient air, they were sealed and kept in vacuum packs. All testing was done in an enclosure filled with dry nitrogen gas, to eliminate moisture uptake or oxidation of the sample. The measured results show no observed changes of the film thickness and density for the nonporous SiCOH after VUV irradiation.

For electrical testing, a hexagonal pattern of titanium (Ti) electrodes was deposited on the dielectric sample using e-beam evaporation, forming a Ti/SiCOH/Cu capacitor. Since the diffusivity of Ti into SiCOH is much smaller than

that of Cu,¹⁵ utilizing Ti electrodes can effectively avoid contamination of low-k dielectrics by Ti during metallization. The area of the electrodes was 3.2×10^{-2} cm² and the thickness was 300 nm. As a control, Ti electrodes were also fabricated on the as-deposited SiCOH thin films.

The C-V characteristics of the Ti/SiCOH/Cu capacitor were measured to examine the dielectric constant of SiCOH after VUV irradiation. The k value of the SiCOH after VUV exposure was calculated to be 3.2 ± 0.1 based on the C-V test results from five samples. Each sample was measured ten times and the measurements were averaged. Compared with the pristine sample (k = 3.2), the k value of SiCOH changes little after VUV exposure. This also shows that the moisture uptake within the material is negligible because absorbed water, with a dielectric constant of ~80, will significantly increase the dielectric constant of the material.¹⁶

To examine Cu diffusion during BTS, an electric field of 2.5 MV/cm, produced with a negative bias on the Ti electrodes, was applied to a Ti/SiCOH/Cu capacitor at a temperature of 225 °C for 5.0 h and 10.0 h, respectively, in an enclosure purged with dry N₂ at atmospheric pressure. The N₂ environment can minimize contamination from moisture or the oxidizing gas from air. That BTS condition was chosen based on two considerations: (1) under 225 °C, the physisorbed water within the SiCOH (water molecules that are hydrogen-bonded to the hydrophilic hydroxyl groups) can be driven out, and meanwhile without harming the integrity of the SiCOH.¹⁷ This further eliminates the impact from absorbed water in the film. (2) The bias, 2.5 MV/cm, is similar to those used in TDDB experiments and models. It is much smaller than the instantaneous hard-breakdown threshold of the Ti/SiCOH/Cu capacitor at 225 °C (4.8 MV/cm). After that, the Ti electrodes were sputtered away using a beam of Ar⁺ ions (E = 3.0 keV) and depth profiles were obtained by scanning over an area of about 1.5 mm × 1.5 mm to ensure a lateral homogeneous ion-current distribution. The sample was rotated during sputtering (E = 1.5 keV) to minimize sputter-induced roughening and the removal rate was about 0.2 nm/s. After each sputter step, Auger electron spectra of the selected elements were recorded.

Figure 2 shows the XPS depth profiles of Cu in both as-deposited and VUV-irradiated SiCOH after BTS. As illustrated in Figure 2(a), after 5.0 h BTS, significant penetration of Cu into the low-k dielectric films was observed: the penetration depth of Cu into the bulk of SiCOH was measured to be 30 nm for the as-deposited sample and 44 nm for the VUV-irradiated sample. The detected Cu profile of the VUV-irradiated sample goes farther into the film for an additional ~14 nm, compared with the as-deposited sample. For the samples that underwent 10.0 h BTS, as illustrated in Figure 2(b), the Cu profile of the VUV-irradiated sample extended an additional ~20 nm farther into the film than that of the as-deposited sample. By using the expression $D_{\text{Cu}} = d^2/2t$, where D_{Cu} is the Cu diffusivity, d is the penetration depth, and t is the temperature stressing time, the estimated diffusivity of Cu at 225 °C was 2.5×10^{-16} cm²/s in the as-deposited sample and was 5.4×10^{-16} cm²/s in the VUV-irradiated sample, which agree with the reported Cu diffusivity in PECVD methyl-doped SiO₂ (SiOCH) at the same temperature.¹⁸ For comparison, Cu profiles in both the as-

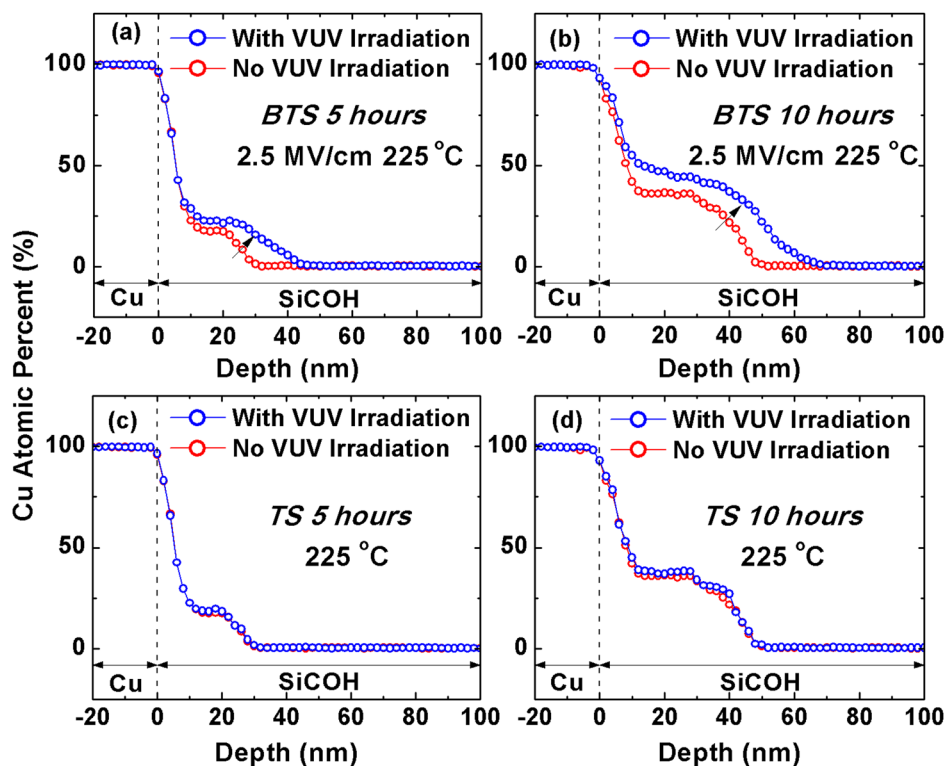


FIG. 2. XPS depth profiles of Cu in as-deposited and VUV-irradiated SiCOH after BTS/TS treatment. (a) 5.0 h BTS and (b) 10.0 h BTS; (c) 5.0 h TS; and (d) 10.0 h TS.

deposited and VUV-irradiated samples under the same temperature-annealing stress without electric bias (TS) were also examined, as shown in Figures 2(c) and 2(d). The samples were annealed at a temperature of 225 °C for 5.0 h and 10.0 h, respectively, with no electric bias applied to the electrodes. Under only TS, the Cu distribution profiles in as-deposited and VUV-irradiated SiCOH are almost the same. It can also be observed that for as-deposited SiCOH, the diffused Cu profiles under BTS are same with that under TS.

These results indicate that the external electric field is able to enhance Cu diffusion into VUV-irradiated SiCOH. Previous work has shown for the diffusion of metallic Cu to be enhanced by the action of an electric field, the Cu must be ionized first.²³ Hence, we postulate that within VUV-irradiated SiCOH, the diffused Cu has been ionized. To further verify this, and to examine the state of diffused Cu within the low-k dielectrics, XPS was performed on both the as-deposited and the VUV irradiated samples. Figure 3 shows the XPS spectra of the Cu 2p core level, which are calibrated with reference to the C 1s peak at 285 eV. The Cu 2p XPS spectrum exhibits two major peaks at binding energies of 932.7 eV and 952.45 eV, which correspond to the Cu 2p_{3/2} and Cu 2p_{1/2} levels, respectively. For the as-deposited sample, the spin-energy separation of the two major peaks (Cu 2p_{3/2} and Cu 2p_{1/2}) is approximately $\Delta_{\text{metal}} = 19.75$ eV, in agreement with other work,^{19,20} revealing that the diffused Cu exists primarily in the atomic state. Two satellite peaks were observed at 964.7 and 945.6 eV for the Cu 2p core-level spectra of VUV-irradiated samples. These satellite peaks reveal the formation of CuO/Cu₂O in the sample, implying that part of the Cu diffused into VUV-irradiated SiCOH is present in ionic form and would interact with the external electric field due to its electropositive characteristic. Since there were no detectable Cu 2p satellite peaks for Cu

diffused into as-deposited SiCOH, we postulate that these changes are induced by VUV irradiation and the source of Cu⁺ available for diffusion is formed via a VUV photon-assisted reaction.

FTIR measurements were made on the samples in an enclosure filled with dry N₂, to examine the characteristic changes in the film after VUV exposure with 9.0 eV photons. The FTIR spectrum in Figure 4 shows that the bond densities of Si-(CH₃)_x (1250–1280 cm⁻¹, 760–870 cm⁻¹), Si-O-Si cage structure with bonding angle $\theta > 144^\circ$ (-1130 cm⁻¹), and C-H_x (2875–2930 cm⁻¹, 760–870 cm⁻¹) structures in as-deposited SiCOH films decreased while the peaks of the Si-O-Si network (1063 cm⁻¹) structures increased after VUV irradiation. These results indicate that a slight carbon loss and a structural rearrangement (i.e., conversion of the Si-O-Si bonds

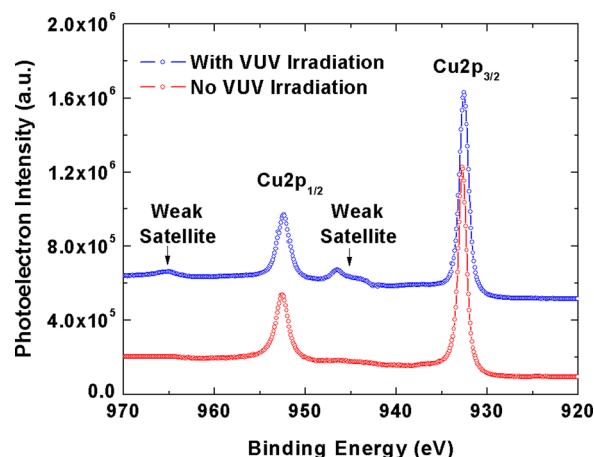


FIG. 3. XPS spectra of Cu 2p core level electron orbitals of diffused Cu in as-deposited and VUV-irradiated SiCOH samples after BTS.

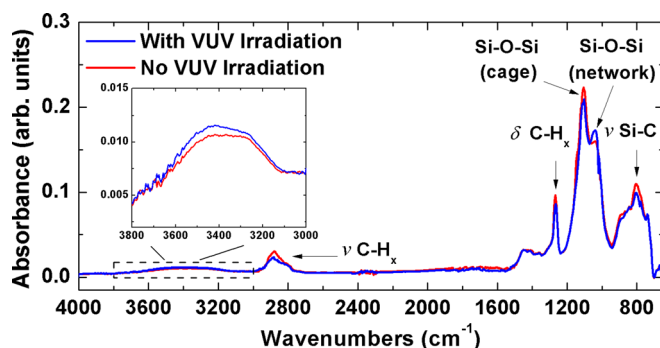


FIG. 4. FTIR spectrum of nonporous SiCOH irradiated by synchrotron with 9.0 eV photons. Here, “ δ ” corresponds to the bending vibrational mode and “ ν ” corresponds to the stretching vibrational mode.

from cage to network) after VUV irradiation, which agrees well with previous results.¹³ Moreover, the broad band at higher wavenumbers of FTIR spectrum, is related to the formation of $-\text{OH}$ groups and to the incorporation of water within the film, i.e., absorbed H_2O ($3300\text{--}3600\text{ cm}^{-1}$), stretching Si-OH ($3200\text{--}3650\text{ cm}^{-1}$), isolated and terminal $-\text{OH}$ ($3650\text{--}3800\text{ cm}^{-1}$).¹⁶ For clarity, the spectra ranging between 3000 and 3800 cm^{-1} are presented in the inset in Figure 4. It is found that after VUV irradiation, the peak intensity of the $-\text{OH}$ related features increases moderately. Since no obvious moisture uptake was observed by measuring the capacitance of the dielectrics as discussed above, the moderate increase of the broad band is believed to result from the formation of $-\text{OH}$ terminals during VUV irradiation.

One significant impact of VUV is loss of silanol ($-\text{OH}$) groups and production of free-radical sites in SiCOH.²¹ Under VUV irradiation, a condensation reaction of two silanol groups can take place within the SiCOH films



Under the combined action of moderate temperatures and an external electric field, the generated negatively charged hydroxyl ions (OH^-) and positively charged hydrogen ions (H^+) are able to diffuse within the dielectric film rapidly due to their higher mobility compared with that of sodium, copper, or other metals.²² Those hydroxyl ions (OH^-) that reach the Cu/dielectric surface may react with Cu to form $\text{Cu}(\text{OH})_2$, which is not stable and can easily decompose to form $\text{CuO}/\text{Cu}_2\text{O}$.²³ These formed metal oxides can become a source of Cu^+ ions that are available for diffusion. It should be noted that the condensation reaction can also produce H_2O . Since the H_2O content within the sample does not increase, as shown by both the C-V and FTIR results, the ionic products of the condensation reaction are the dominant oxidation species. Under BTS there are two driving forces for Cu^+ migration: diffusion caused by a concentration gradient and drift caused by an electric field. Thus, the migration process of positively charged Cu^+ in VUV-irradiated SiCOH will be accelerated; while for Cu existing as atomic states, the electrostatic acceleration would be negligible since it is electrically neutral. This explains why VUV-irradiated SiCOH has a larger calculated Cu diffusivity and shows a larger Cu penetration depth than that for the as-deposited SiCOH, even though the BTS conditions are the

same; while under the same TS condition, the profiles of diffused Cu remain the same for both samples.

To verify this, the same BTS/TS treatment was made on the SiCOH/no plasma pre-cleaned Cu film stack. Since the Cu films were not treated by plasma before deposition of SiCOH on it, Cu corrosion inhibitors left behind by the Cu CMP process and Cu surface oxides formed by ambient exposure existing at the Cu/SiCOH interface can become a source of Cu^+ ions with the appearance of an external electrical field. It was found in the Cu/no plasma pre-clean/SiCOH sample, under BTS, the Cu penetration depth is larger than that for those samples treated only by TS. This agrees well with the results for the VUV-irradiated samples and further verifies the Cu oxidation in VUV-irradiated SiCOH. We also note that Cu profiles under BTS/TS in either as-deposited or VUV-irradiated SiCOH come with “humps” at shallow depth. These humps have been previously observed by He *et al.*¹⁰ and are believed to be related to Cu diffusion kinetics and solubility in SiCOH. Future work is planned to clarify the impact of VUV irradiation on Cu diffusion kinetics and solubility in SiCOH.

In conclusion, VUV irradiation was found to be able to affect copper penetration into low-k porous dielectrics under bias-temperature stress. Further analysis shows this effect is correlated with the number of hydroxyl free-radical sites generated by VUV photon irradiation in the dielectrics. These results suggest that the role of VUV photons may need to be considered in studying the interactions between Cu and low-k dielectrics. The reliability of the Cu/low-k dielectric interface is still a challenge for successful integration of Cu with low-k interlayer dielectrics.

This work was supported by the Semiconductor Research Corporation under Contract No. 2012-KJ-2359 and by the National Science Foundation under Grant No. CBET-1066231.

¹International Technology Roadmap for Semiconductors (ITRS), Semiconductor Industry Association, San Jose, CA, 2009.

²E. Besien, M. Pantouvaki, L. Zhao, D. De Roest, M. Baklanov, Z. Tokei, and G. Beyer, *Microelectron. Eng.* **92**, 59 (2012).

³J. Lloyd, E. Liniger, and T. Shaw, *J. Appl. Phys.* **98**, 84109 (2005).

⁴R. H. Havemann and J. A. Hutchby, *Proc. IEEE* **89**, 586 (2001).

⁵J. Atkin, E. Cartier, T. Shaw, R. Laibowitz, and T. Heinz, *Appl. Phys. Lett.* **93**, 122902 (2008).

⁶J. Atkin, D. Song, T. Shaw, E. Cartier, R. Laibowitz, and T. Heinz, *J. Appl. Phys.* **103**, 094104 (2008).

⁷S. Uchida, S. Takashima, M. Hori, M. Fukasawa, K. Ohshima, K. Nagahata, and T. Tatsumi, *J. Appl. Phys.* **103**, 073303 (2008).

⁸M. T. Nichols, H. Sinha, C. A. Wiltbank, G. A. Antonelli, Y. Nishi, and J. L. Shohet, *Appl. Phys. Lett.* **100**, 112905 (2012).

⁹B. Jinnai, T. Nozawa, and S. Samukawa, *J. Vac. Sci. Technol., B* **26**, 1926 (2008).

¹⁰M. He, S. Novak, L. Vanamurthy, H. Bakhr, J. Plawsky, and T. M. Lu, *Appl. Phys. Lett.* **97**, 252901 (2010).

¹¹S. King, M. French, M. Jaehnic, M. Kunh, and B. French, *Appl. Phys. Lett.* **99**, 202903 (2011).

¹²S. King, B. French, and E. Mays, *J. Appl. Phys.* **113**, 044109 (2013).

¹³X. Guo, J. E. Jakes, S. Banna, Y. Nishi, and J. L. Shohet, *J. Appl. Phys.* **116**, 044103 (2014).

¹⁴J. R. Woodworth, M. E. Riley, V. A. Amatucci, T. W. Hamilton, and B. P. Aragon, *J. Vac. Sci. Technol. A* **19**, 45 (2001).

¹⁵J. D. McBrayer, R. M. Swanson, and T. W. Sigmon, *J. Electrochem. Soc.* **133**, 1242 (1986).

- ¹⁶X. Guo, J. E. Jakes, M. T. Nichols, S. Banna, Y. Nishi, and J. L. Shohet, *J. Appl. Phys.* **114**, 084103 (2013).
- ¹⁷Y. Li, I. Ciofi, L. Carbonell, N. Heylen, J. V. Aelst, M. R. Baklanov, G. Groeseneken, K. Maex, and Z. Tokei, *J. Appl. Phys.* **104**, 034113 (2008).
- ¹⁸K. S. Kim, Y. C. Joo, K. B. Kim, and J. Y. Kwon, *J. Appl. Phys.* **100**, 063517 (2006).
- ¹⁹J. Ghijsen, L. H. Tjeng, J. V. Elp, H. Eskes, J. Westerink, G. A. Sawatzky, and M. T. Czyzyk, *Phys. Rev. B* **38**, 11322 (1988).
- ²⁰M. Yin, C. Wu, Y. Lou, C. Burda, J. T. Koberstein, Y. Zhu, and S. O'Brien, *J. Am. Chem. Soc.* **127**, 9506 (2005).
- ²¹F. Iacopi, Y. Travaly, B. Eyckens, C. Waldfried, T. Abell, E. P. Guyer, D. M. Gage, R. H. Dauskardt, T. Sajavaara, K. Houthoofd, P. Grobet, P. Jacobs, and K. Maex, *J. Appl. Phys.* **99**, 053511 (2006).
- ²²A. B. Duso and D. Y. Chen, *Anal. Chem.* **74**, 2938 (2002).
- ²³O. R. Rodriguez, W. Cho, R. Saxena, J. L. Plawsky, and W. N. Gill, *J. Appl. Phys.* **98**, 024108 (2005).